JACS
JOURNAL OF THE AMERICAN CHEMICAL SOCIETY
Communication
pubs.acs.org/JACS

Metal–Organic Framework-Immobilized Polyhedral Metal Nanocrystals: Reduction at Solid–Gas Interface, Metal Segregation, Core–Shell Structure, and High Catalytic Activity

Arshad Aijaz,[†] Tomoki Akita,[†] Nobuko Tsumori,[‡] and Qiang Xu*[,†]

[†]National Institute of Advanced Industrial Science and Technology (AIST), Ikeda, Osaka 563-8577, Japan
[‡]Toyama National College of Technology, 13 Hongo-machi, Toyama, 939-8630, Japan

Supporting Information

ABSTRACT: For the first time, this work presents surfactant-free monometallic and bimetallic polyhedral metal nanocrystals (MNCs) immobilized to a metal–organic framework (MIL-101) by CO-directed reduction of metal precursors at the solid–gas interface. With this novel method, Pt cubes and Pd tetrahedra were formed by CO preferential bindings on their (100) and (111) facets, respectively. PtPd bimetallic nanocrystals showed metal segregation, leading to Pd-rich core and Pt-rich shell. Core–shell Pt@Pd nanocrystals were immobilized to MIL-101 by seed-mediated two-step reduction, representing the first example of core–shell MNCs formed using only gas-phase reducing agents. These MOF-supported MNCs exhibited high catalytic activities for CO oxidation.

The fascinating mono- and bimetallic polyhedral nanocrystals have attracted growing attention owing to their unique properties, which are different from those of their spherical counterparts,[1] and have been extensively used in a wide range of applications, such as catalysis including reforming of hydrocarbons and reduction of oxygen in fuel cells, sensing of biomolecules, enhancing spectral signals, photothermal therapy, and so on.[2] Recent works have shown that the catalytic activity and selectivity of such catalysts can be altered significantly by the nature of the metal facets exposed to reactants.[3] In general, polyhedral MNCs are prepared by wet-chemical approaches in colloidal solutions with the use of surfactant/capping agents.[4] Very recently, carbon monoxide (CO) gas has been used to generate specific facets in solution-phase reactions containing polyvinylpyrrolidone/oleylamine/oleic acid.[5] However, in such approaches, excessive amounts of organic agents are employed, often leading to contamination problems, and as the catalytic process takes place on the metal surfaces, the presence of a protective organic shell around the MNCs is unfavorable for catalytic applications. Therefore, a suitable approach that can overcome such problems is demanded.

Metal–organic frameworks (MOFs), a new class of crystalline porous materials, have predesignable pore structures and promising multifunctionalities.[6] Over the past decade, research efforts have been mostly aimed at preparing new MOF structures and studying their applications in molecule storage and separation.[7] Given the similarity to zeolites, depositing metal nanoparticles to MOFs could afford heterogeneous catalysts.[8−10] It is expected that the crystalline porous structures of MOFs limit the migration and aggregation of metal nanoparticles. So far, there are some examples of MOF-supported sphere-shaped mono- and bimetallic nanoparticles but only one example, to the best of our knowledge, of MOF-immobilized core–shell metal nanoparticles, which were prepared by the wet-chemical approach,[10b] whereas no polyhedral MNCs supported on MOFs have been reported. Furthermore, notably no examples of surfactant-free core–shell metal nanoparticles/nanocrystals formed by gas-phase reduction have been reported. Herein, we report for the first time that polyhedral MNCs can be successfully immobilized to MIL-101, a representative MOF, by direct reduction of metal precursors at the solid–gas interface without use of any surfactant/liquid-capping agents (Scheme 1).

Scheme 1. Schematic Illustration of the Formation of Cubic Pt, Tetrahedral Pd, and Octahedral PtPd Metal Nanocrystals on MIL-101 Support in the Presence of CO and H_2

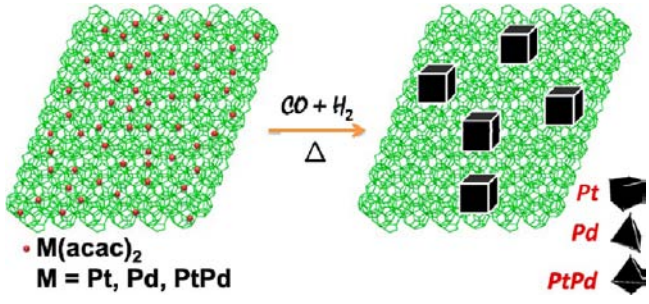

Polyhedral bimetallic PtPd nanocrystals having a core–shell-like structure with a Pt-rich shell have been formed because of the segregation effect in the one-step CO-directed reduction process, while Pt@Pd core–shell nanocrystals have been synthesized by a seed-mediated two-step reduction. The whole reduction processes have been carried out under dry conditions using only gas-phase reducing agents.

MIL-101, a chromium-based MOF with molecular formula $Cr_3F(H_2O)_2O[(O_2C)C_6H_4(CO_2)]_3{\cdot}nH_2O$ (where n is ~25), has been used as the support, which has high stability, large surface area, and two zeotypic cavities with diameters of 2.9 and 3.4 nm accessible through two pore windows of 1.2 and 1.6 nm.[7g]

Received: September 8, 2013
Published: October 18, 2013

dx.doi.org/10.1021/ja4093055 | J. Am. Chem. Soc. 2013, 135, 16356–16359

MIL-101 supported MNCs were prepared by using a CO/H_2/He mixture as gas-phase reducing agents. Briefly, metal acetylacetonate, $M(acac)_2$ (M = Pt, Pd or Pt/Pd), was first dissolved in a mixture of acetone/DMF (1:1), impregnated into a preactivated MIL-101 support by incipient wetness method, and then dried under a vacuum at 70 °C for overnight. The solids were subsequently heated to 200 °C in a stream of CO/H_2/He (40/10/50 mL min^{-1}) for 1 h to produce Pt/MIL-101, Pd/MIL-101, and PtPd/MIL-101.[11] There was no loss of crystallinity in the powder X-ray diffraction (PXRD) patterns after reduction, suggesting that the integrity of the MIL-101 framework was maintained after MNCs deposition (Figure S1, Supporting Information (SI)). Very weak diffractions for a face-centered cubic (fcc) structure were detected for Pt, Pd, and PtPd nanocrystals from powder XRD patterns, which might be due to the low metal loadings. The decreases in the amount of N_2 adsorption and the pore volume of these samples indicate that the cavities of the host framework are occupied by dispersed MNCs and/or blocked by the MNCs located at the surface (Figure S2 (SI)), as observed in the cases of loading metal nanoparticles to ZIF-8, MOF-5, and other porous materials.[8] The X-ray photoelectron spectra (XPS) of Pt/MIL-101, Pd/MIL-101 and PtPd/MIL-101 at the Pt 4f and Pd 3d levels exhibit metallic Pt and Pd peaks (Figures S3–S5 (SI)); Ar etching of PtPd/MIL-101 for 240 min reveals a Pt-rich shell (Figure S5 (SI)). High-angle annular dark field (HAADF) and bright field (BF) scanning transmission electron microscopy (STEM) images reveal majority of cubic Pt (Figure 1a), tetrahedral Pd

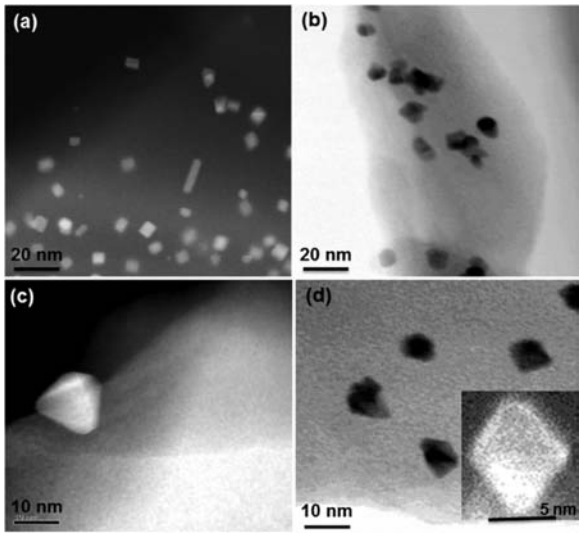

Figure 1. STEM images of (a) Pt/MIL-101, (b, c) Pd/MIL-101, and (d) PtPd/MIL-101. Inset in (d) shows a single octahedron.

(Figure 1b and 1c) and PtPd octahedral (Figure 1d) nanocrystals deposited to MIL-101.[11] Statistical analysis of the images by counting the numbers of MNCs with different shapes (Figures 1 and S6–S8 (SI)) show that most of the MNCs are cubic (88%), tetrahedral (80%), and octadedral (65%) with average sizes of 8.0, 8.5, and 10.5 nm in Pt/MIL-101, Pd/MIL-101 and PtPd/MIL-101, respectively. The cubic Pt nanocrystals have straight edges with sharp corners, while the tetrahedral Pd and octahedral PtPd nanocrystals have straight edges with little truncated corners. The byproducts in Pt/MIL-101 consist of some spheres, rectangular structures and rods, whereas Pd/MIL-101 and PtPd/MIL-101 contain only some spheric, prismatic, and multifaceted polyhedral nanocrystals.

Energy-dispersive X-ray spectroscopy (EDS) elemental mapping of PtPd nanocrystal showes a Pt-rich shell with a PtPd bimetallic core, in agreement with the XPS observations (Figure 2). Because the adsorption enthalpy of CO on Pt is

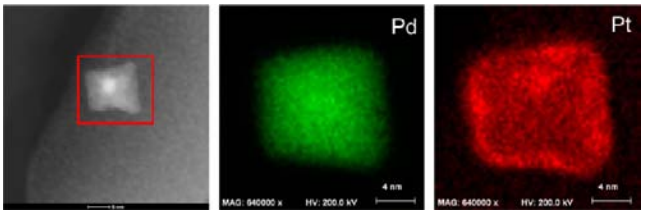

Figure 2. HAADF-STEM image of single PtPd nanocrystal deposited on MIL-101 with corresponding EDS Pd-L and Pt-M mapping images.

higher than on Pd, Pt segregates to the surface of the nanocrystals and correspondingly displaces Pd to the core, leading to a Pd-rich core with a Pt-rich shell.[12] Such adsorbate-induced surface segregation in MNPs are highly demanded in heterogeneous catalysis, which can reduce the use of expensive Pt for better catalytic activity.[12b] To the best of our knowledge, it is the first example of metal segregation observed for MOF-supported MNPs, providing new possibilities for MOF-based catalysts.

Single-crystal seeds are believed to grow from tiny clusters that are generated through self-nucleation during the initial stage of synthesis. The final size and shape of the MNCs are then decided by the reducing/capping agents.[1d] It is well-known that the capping agents are used to stabilize certain facets through selective chemisorption, and as a result, the growth rates of various types of facets are altered, leading to the formation of MNCs with diversified shapes. CO, working as a capping agent, preferentially binds to specific surfaces of metals, leading to the formation of polyhedral MNCs.[1d] It is found that the use of H_2/He in place of CO/H_2/He under the same experimental conditions results in spherical Pt (Figure S9 (SI)), suggesting that CO directs the growth of Pt and shapes them into cubes. The formation of a cubic shape is likely associated with preferential chemisorption of CO on Pt (100), thereby modifying the growth kinetics.[5c] Previous experimental and theoretical studies have shown stronger binding of CO molecules to Pt (100) than to other low-indexed facets.[13] The strongly adsorbed CO will inhibit the growth of (100) planes, making these planes the bounding surfaces of the final MNCs. Similarly, tetrahedral Pd nanocrystals, which are enclosed with (111) facets, are results of preferential chemisorption of CO on Pd(111) facets.

Seed-mediated growth has emerged as one of the most effective routes to the synthesis of core–shell MNCs in colloidal solutions, by which the size, structure, and morphology of resultant MNCs can be tailored in a controllable fashion.[14] In general, solution-phase seed-mediated growth involves two major steps: (i) synthesis of seeds with uniform and relatively small sizes and (ii) nucleation and growth of another metal on the as-prepared seeds, leading to the formation of core–shell MNCs. In this work, to obtain core–shell Pt@Pd nanocrystals, the two-step reduction process has been adopted, but under dry reduction condition by the use of gas-phase reducing agent. As shown in Scheme 2, small spherical Pt were used as seeds (core) for the growth of Pd shell. Typically, Pt seeds with an average size of 2 nm immobilized to MIL-101 (Figure S10 (SI)) were first synthesized by reducing the H_2PtCl_6 impregnated MIL-101 in

dx.doi.org/10.1021/ja4093055 | J. Am. Chem. Soc. 2013, 135, 16356–16359

Scheme 2. Schematic Illustration of the Formation of Pt@Pd Core–Shell Tetrahedral MNCs on MIL-101 Support in the Presence of CO and H_2

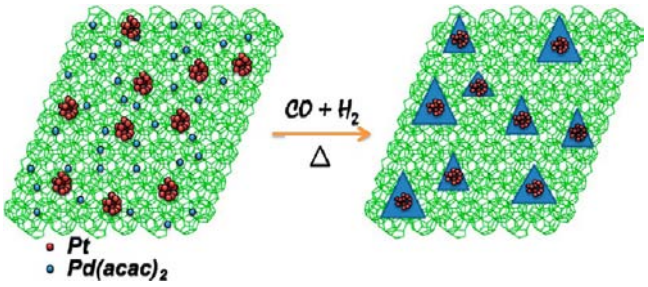

the mixture of $CO/H_2/He$ (40/10/50 mL min^{-1}) at 200 °C for 1 h. $Pd(acac)_2$ dissolved in DMF/acetone was added dropwisely onto the resultant sample under continuous stirring, dried in a vacuum, and then reduced in a $CO/H_2/He$ (40/10/50 mL min^{-1}) flow at 200 °C for 1 h, leading to the formation of Pt@Pd/MIL-101.[11] N_2 adsorption (Figure S11 (SI)) and PXRD (Figure S12 (SI)) measurements confirmed the stability of MIL-101 framework.

Transmission electron microscopy (TEM) (Figure 3a) and HAADF-STEM (Figures 3b,c) observations of Pt@Pd/MIL-101

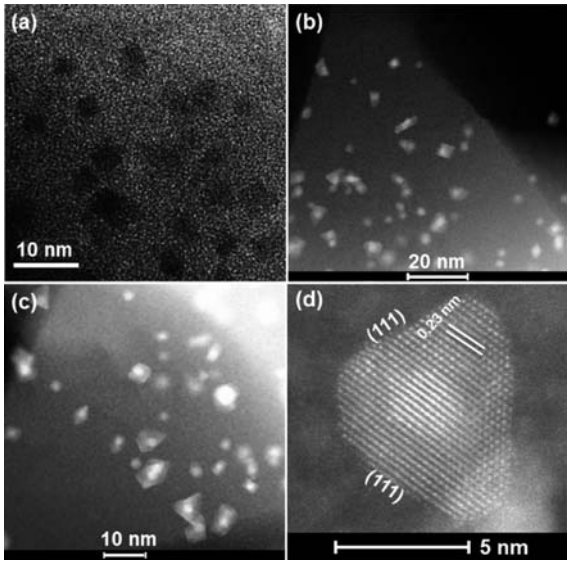

Figure 3. (a) TEM, (b, c) HAADF-STEM, and (d) high resolution HAADF-STEM of Pt@Pd/MIL-101.

revealed uniform distribution of polyhedral MNCs with sizes of 3–9 nm to MIL-101 framework. Most of them (~70%) are either tetrahedron- or truncated tetrahedron-shaped nanocrystals with some spheres, cubes, rectangles, and octahedra as byproducts. A bright spherical core (Pt) coated by a darker shell (Pd) is observed for each particle in the HAADF-STEM images (Figures 3d and S13 (SI)). The distance between adjacent lattice fringes (Figure 3d) in the Pd shell is ~0.23 nm, which fits well the distance between the (111) planes of the fcc Pd. The single Pt@Pd nanocrystal projected along the ⟨110⟩ zone axis shows two (111) facets with characteristic fast Fourier transform (FFT) pattern, indicating that the nanocrystal is a tetrahedron truncated by (111) and (100) planes (Figure S14 (SI)). Relative to Pd nanocubes, the formation of Pd nanocrystals with surface enclosed by (111) facets should be more favored because of their lower surface energy. Also, CO adsorbs selectively on Pd(111) facets, which retards the continuous growth of these faces with minimum surface energy, resulting in the majority of tetrahedron-shaped core–shell Pt@Pd nanocrystals enclosed with (111) facets.

It has been reported that Pt(100) and Pd(111) facets are the most active surfaces for CO oxidation reaction, because of the appropriate CO adsorption strength.[15] This catalytic reaction, important in automobile emission control, is known to be sensitive to the structure of the MNCs.[3a] We have investigated our MNCs deposited to MIL-101 as model catalysts for CO oxidation reaction. The reaction was performed using a fixed bed flow reactor from room to elevated temperatures.[11] Figure 4

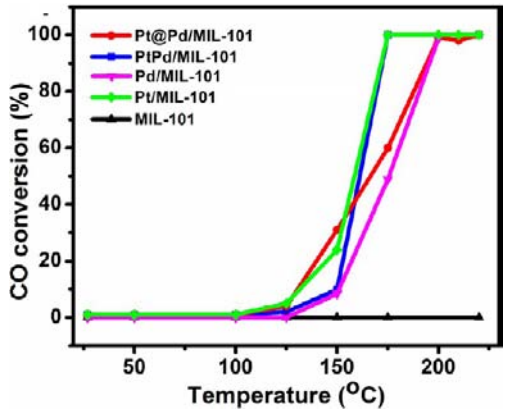

Figure 4. Conversion of CO over MIL-101 and MIL-101-supported MNC catalysts as a function of temperature ($CO:O_2:He$ = 1:20:79, 20 000 mL h^{-1} g_{cat}^{-1}).

shows the CO conversion as a function of temperature. MIL-101 exhibited no catalytic activity for CO oxidation reaction in the whole temperature range. All the MNC catalysts were found to be highly active for CO conversion to CO_2. Pt/MIL-101, PtPd/MIL-101, and Pt@Pd/MIL-101 started to show the activity at 100 °C, while CO to CO_2 conversion increased suddenly at 150 °C with complete conversion at 175, 175, and 200 °C, respectively. However, Pd/MIL-101 started to show the activity at 125 °C with complete conversion at 200 °C. Arrhenius plots show that the activation energies for Pt/MIL-101, Pd/MIL-101, PtPd/MIL-101, and Pt@Pd/MIL-101 are 69.0, 77.8, 72.7, and 62.6 kJ mol^{-1}, respectively (Figure S15 (SI)), which are comparable to the reported values of the other MOF-supported fine metal nanocatalysts for CO oxidation.[16] In comparison with other samples, Pd/MIL-101 showed slightly larger activation energy and higher temperature for starting to show CO conversion to CO_2, corresponding to slightly lower catalytic activity for CO oxidation. After catalytic reactions, the crystallinities of MIL-101 frameworks remain unchanged, as confirmed by the PXRD patterns (Figure S16 (SI)). The small sub-10 nm sizes of the MNCs stably immobilized to MIL-101 frameworks with exposed Pt(100) and Pd(111) facets largely contribute to the high catalytic activities of these catalysts.

In summary, for the first time, mono- and bimetallic surfactant-free polyhedral MNCs were immobilized to a porous MOF by a facile CO-directed reduction method at solid–gas interface. The first observations of metal segregation and core–shell polyhedral structure of MNCs on MOFs under gas-phase reduction conditions are encouraging, which might open up a new avenue in the development of MNCs with different shapes and

dx.doi.org/10.1021/ja4093055 | J. Am. Chem. Soc. 2013, 135, 16356–16359

compositions as superior heterogeneous catalysts by using MOFs as well as other porous materials as supports.

■ ASSOCIATED CONTENT

Supporting Information

Experimental details, characterization data, additional STEM images. This material is available free of charge via the Internet at http://pubs.acs.org.

■ AUTHOR INFORMATION

Corresponding Author

q.xu@aist.go.jp

Notes

The authors declare no competing financial interest.

■ ACKNOWLEDGMENTS

The authors are thankful to the reviewers for valuable suggestions, Ms. Chie Fukada for assistance in TEM measurements, and AIST and JSPS for financial support. N.T. thanks JSPS (No.25420829) for financial support and Ms. Marina Yamamoto for assistance in CO oxidation experiments. A.A. thanks JSPS for a postdoctoral fellowship.

■ REFERENCES

(1) (a) Chen, M.; Wu, B.; Yang, J.; Zheng, N. *Adv. Mater.* **2012**, *24*, 862. (b) Zhou, K.; Li, Y. *Angew. Chem., Int. Ed.* **2012**, *51*, 602. (c) Zhou, Z.-Y.; Tian, N.; Li, J.-T.; Broadwell, I.; Sun, S.-G. *Chem. Soc. Rev.* **2011**, *40*, 4167. (d) Xia, Y.; Xiong, Y.; Lim, B.; Skrabalak, S. E. *Angew. Chem., Int. Ed.* **2009**, *48*, 60. (e) Grzelczak, M.; Pérez-Juste, J.; Mulvaney, P.; Liz-Marzán, L. M. *Chem. Soc. Rev.* **2008**, *37*, 1783. (f) Tao, A. R.; Habas, S.; Yang, P. *Small* **2008**, *4*, 310. (g) Xiong, Y.; Xia, Y. *Adv. Mater.* **2007**, *19*, 3385.

(2) (a) Wang, D.; Xin, H. L.; Hovden, R.; Wang, H.; Yu, Y.; Muller, D. A.; DiSalvo, F. J.; Abruña, H. D. *Nat. Mater.* **2013**, *12*, 81. (b) Zhang, H.; Jin, M.; Xia, Y. *Chem. Soc. Rev.* **2012**, *41*, 8035. (c) Peng, Z.; Kisielowski, C.; Bell, A. T. *Chem. Commun.* **2012**, *48*, 1854. (d) Huang, X. H.; Neretina, S.; El-Sayed, M. A. *Adv. Mater.* **2009**, *21*, 4880. (e) Gordon, R.; Sinton, D.; Kavanagh, K. L.; Brolo, A. G. *Acc. Chem. Res.* **2008**, *41*, 1049. (f) Gobin, A. M.; Lee, M. H.; Halas, N. J.; James, W. D.; Drezek, R. A.; West, J. L. *Nano Lett.* **2007**, *7*, 1929.

(3) (a) Xie, X.; Li, Y.; Liu, Z.-Q.; Haruta, M.; Shen, W. *Nature* **2009**, *458*, 746. (b) Somorjai, G. A.; Frei, H.; Park, J. Y. *J. Am. Chem. Soc.* **2009**, *131*, 16589. (c) Stamenkovic, V. R.; Fowler, B.; Mun, B. S.; Wang, G. F.; Ross, P. N.; Lucas, C. A.; Markovic, N. M. *Science* **2007**, *315*, 493. (d) Bratlie, K. M.; Lee, H.; Komvopoulos, K.; Yang, P.; Somorjai, G. A. *Nano Lett.* **2007**, *7*, 3097.

(4) (a) Zhang, J.; Yang, H. Z.; Fang, J. Y.; Zou, S. H. *Nano Lett.* **2010**, *10*, 638. (b) Cozzoli, P. D.; Pellegrino, T.; Manna, L. *Chem. Soc. Rev.* **2006**, *35*, 1195.

(5) (a) Mourdikoudis, S.; Liz-Marzán, L. M. *Chem. Mater.* **2013**, *25*, 1465. (b) Dai, Y.; Mu, X.; Tan, Y.; Lin, K.; Yang, Z.; Zheng, N.; Fu, G. *J. Am. Chem. Soc.* **2012**, *134*, 7073. (c) Huang, X.; Tang, S.; Mu, X.; Dai, Y.; Chen, G.; Zhou, Z.; Ruan, F.; Yang, Z.; Zheng, N. *Nat. Nanotechnol.* **2011**, *6*, 28. (d) Wu, J.; Gross, A.; Yang, H. *Nano Lett.* **2011**, *11*, 798. (e) Kang, Y. J.; Ye, X. C.; Murray, C. B. *Angew. Chem., Int. Ed.* **2010**, *49*, 6156.

(6) (a) Yoon, M.; Srirambalaji, R.; Kim, K. *Chem. Rev.* **2012**, *112*, 1196. (b) Li, J.-R.; Sculley, J.; Zhou, H.-C. *Chem. Rev.* **2012**, *112*, 869. (c) Chen, B.; Xiang, S.; Qian, G. *Acc. Chem. Res.* **2010**, *43*, 1115. (d) Farha, O. K.; Hupp, J. T. *Acc. Chem. Res.* **2010**, *43*, 1166. (e) Long, J. R.; Yaghi, O. M. *Chem. Soc. Rev.* **2009**, *38*, 1213. (f) Férey, G. *Chem. Soc. Rev.* **2008**, *37*, 191. (g) Kitagawa, S.; Kitaura, R.; Noro, S. *Angew. Chem., Int. Ed.* **2004**, *43*, 2334.

(7) (a) Sen, S.; Nair, N. N.; Yamada, T.; Kitagawa, H.; Bharadwaj, P. K. *J. Am. Chem. Soc.* **2012**, *134*, 19432. (b) Furukawa, H.; Ko, N.; Go, Y. B.; Aratani, N.; Choi, S. B.; Choi, E.; Yazaydin, A. Ö.; Snurr, R. Q.; O'Keeffe, M.; Kim, J.; Yaghi, O. M. *Science* **2010**, *329*, 424. (c) Jiang, H.-L.; Tastu, Y.; Lu, Z.-H.; Xu, Q. *J. Am. Chem. Soc.* **2010**, *132*, 5586. (d) Xiang, S. C.; Zhou, W.; Gallegos, J. M.; Liu, Y.; Chen, B. *J. Am. Chem. Soc.* **2009**, *131*, 12415. (e) Mulfort, K. L.; Hupp, J. T. *J. Am. Chem. Soc.* **2007**, *129*, 9604. (f) Pan, L.; Parker, B.; Huang, X. Y.; Olson, D. H.; Lee, J.; Li, J. *J. Am. Chem. Soc.* **2006**, *128*, 4180. (g) Férey, G.; Mellot-Draznieks, C.; Serre, C.; Millange, F.; Dutour, J.; Surblé, S.; Margiolaki, I. *Science* **2005**, *309*, 2040. (h) Seo, J. S.; Whang, D.; Lee, H.; Jun, S. I.; Oh, J.; Jeon, Y. J.; Kim, K. *Nature* **2000**, *404*, 982.

(8) (a) Dhakshinamoorthy, A.; Garcia, H. *Chem. Soc. Rev.* **2012**, *41*, 5262. (b) Meilikhov, M.; Yusenko, K.; Esken, D.; Turner, S.; Tendeloo, G. V.; Fischer, R. A. *Eur. J. Inorg. Chem.* **2010**, *24*, 3701.

(9) (a) Aijaz, A.; Karkamkar, A.; Choi, Y. J.; Tsumori, N.; Ronnebro, E.; Autrey, T.; Shioyama, H.; Xu, Q. *J. Am. Chem. Soc.* **2012**, *134*, 13926. (b) Kong, G.-Q.; Ou, S.; Zou, C.; Wu, C.-D. *J. Am. Chem. Soc.* **2012**, *134*, 19851. (c) Lu, G.; Li, S. Z.; Guo, Z.; Farha, O. K.; Hauser, B. G.; Qi, X. Y.; Wang, Y.; Wang, X.; Han, S. Y.; Liu, X. G.; DuChene, J. S.; Zhang, H.; Zhang, Q. C.; Chen, X. D.; Ma, J.; Loo, S. C. J.; Wei, W. D.; Yang, Y. H.; Hupp, J. T.; Huo, F. W. *Nat. Chem.* **2012**, *4*, 310. (d) Wang, C.; Dekrafft, K. E.; Lin, W. *J. Am. Chem. Soc.* **2012**, *134*, 7211. (e) Park, T.-H.; Hickman, A. J.; Koh, K.; Martin, S.; Wong-Foy, A. G.; Sanford, M. S.; Matzger, A. J. *J. Am. Chem. Soc.* **2011**, *133*, 20138. (f) Park, Y. K.; Choi, S. B.; Nam, H. J.; Jung, D.-Y.; Ahn, H. C.; Choi, K.; Furukawa, H.; Kim, J. *Chem. Commun.* **2010**, *46*, 3086. (g) Esken, D.; Turner, S.; Lebedev, O. I.; Tendeloo, G. V.; Fischer, R. A. *Chem. Mater.* **2010**, *22*, 6393. (h) Cheon, Y. E.; Suh, M. P. *Angew. Chem., Int. Ed.* **2009**, *48*, 2899. (i) Schröder, F.; Esken, D.; Cokoja, M.; van den Berg, M. W. E.; Lebedev, O. I.; Tendeloo, G. V.; Walaszek, B.; Buntkowsky, G.; Limbach, H.-H.; Chaudret, B.; Fischer, R. A. *J. Am. Chem. Soc.* **2008**, *130*, 6119. (j) Hwang, Y. K.; Hong, D.-Y.; Chang, J.-S.; Jhung, S. H.; Seo, Y.-K.; Kim, J.; Vimont, A.; Daturi, M.; Serre, C.; Férey, G. *Angew. Chem., Int. Ed.* **2008**, *47*, 4144.

(10) (a) Zhu, Q.-L.; Li, J.; Xu, Q. *J. Am. Chem. Soc.* **2013**, *135*, 10210. (b) Jiang, H. L.; Akita, T.; Ishida, T.; Haruta, M.; Xu, Q. *J. Am. Chem. Soc.* **2011**, *133*, 1304. (c) Ameloot, R.; Roeffaers, M. B. J.; De Cremer, G.; Vermoortele, F.; Hofkens, J.; Sels, B. F.; De Vos, D. E. *Adv. Mater.* **2011**, *23*, 1788. (d) Li, H.; Zhu, Z.; Zhang, F.; Xie, S.; Li, H.; Li, P.; Zhou, X. *ACS Catal.* **2011**, *1*, 1604. (e) Zlotea, C.; Campesi, R.; Cuevas, F.; Leroy, E.; Dibandjo, P.; Volkringer, C.; Loiseau, T.; Férey, G.; Latroche, M. *J. Am. Chem. Soc.* **2010**, *132*, 2991. (f) Samy El-Shall, M.; Abdelsayed, V.; Khder, A. S.; Hassan, H. M. A.; El-Kaderi, H. M.; Reich, T. E. *J. Mater. Chem.* **2009**, *19*, 7625. (g) Jiang, H.-L.; Liu, B.; Akita, T.; Haruta, M.; Sakurai, H.; Xu, Q. *J. Am. Chem. Soc.* **2009**, *131*, 11302. (h) Proch, S.; Herrmannsdörfer, J.; Kempe, R.; Kern, C.; Jess, A.; Seyfarth, L.; Senker, L. *Chem.—Eur. J.* **2008**, *14*, 8204. (i) Henschel, A.; Gedrich, K.; Kraehnert, R.; Kaskel, S. *Chem. Commun.* **2008**, 4192. (j) Ishida, T.; Nagaoka, M.; Akita, T.; Haruta, M. *Chem.—Eur. J.* **2008**, *14*, 8456.

(11) See the Supporting Information.

(12) (a) Fischer-Wolfarth, J.-H.; Farmer, J. A.; Flores-Camacho, J. M.; Genest, A.; Yudanov, I. V.; Rösch, N.; Campbell, C. T.; Schauermann, S.; Freund, H.-J. *Phys. Rev. B* **2010**, *81*, 24141. (b) Mayrhofer, K. J. J.; Juhart, V.; Hartl, K.; Hanzlik, M.; Arenz, M. *Angew. Chem., Int. Ed.* **2009**, *48*, 3529.

(13) Palaikis, L.; Zurawski, D.; Hourani, M.; Wieckowski, A. *Surf. Sci.* **1988**, *199*, 183.

(14) (a) DeSantis, C. J.; Skrabalak, S. E. *J. Am. Chem. Soc.* **2013**, *135*, 10. (b) Niu, W.; Zhang, L.; Xu, G. *Nanoscale* **2013**, *5*, 3172. (c) Langille, M. R.; Zhang, J.; Personick, M. L.; Li, S.; Mirkin, C. A. *Science* **2012**, *337*, 954. (d) Habas, S. E.; Lee, H.; Radmilovic, V.; Somorjai, G. A.; Yang, P. D. *Nat. Mater.* **2007**, *6*, 692. (e) Jana, N. R.; Gearheart, L.; Murphy, C. *J. Chem. Mater.* **2001**, *13*, 231.

(15) Wang, R.; He, H.; Wang, J.; Liu, L.; Dai, H. *Catal. Today* **2013**, *201*, 68.

(16) (a) Ye, J.-Y.; Liu, C.-J. *Chem. Commun.* **2011**, *47*, 2167. (b) Samy El-Shall, M.; Abdelsayed, V.; Khder, A. S.; Hassan, H. M. A.; El-Kaderi, H. M.; Reich, T. E. *J. Mater. Chem.* **2009**, *19*, 7625.